Effect of d electrons in transition-metal ions on band-gap energies of diluted magnetic semiconductors

Y. D. Kim, Yia-Chung Chang, and M. V. Klein
Department of Physics and Materials Research Laboratory, University of Illinois at Urbana-Champaign, 1110 West Green Street, Urbana, Illinois 61801
(Received 19 July 1993)

We present a theoretical study of the effect of partially filled d electrons in transition-metal ions on the E_1 and $E_1+\Delta_1$ band-gap energies of the diluted magnetic semiconductors. Semiempirical tight-binding calculations were performed to study the effects of interactions arising from the hybridization between the localized d orbitals of a transition-metal impurity and the bulk band states of II-VI semiconductors on the Γ- and L-point band gaps. Our results account for the concentration dependence of the L-point band gaps in the $Zn_{1-x}(Mn,Fe,Co)_xSe$ system in the range of small x. The effect of this hybridization strongly depends on the location of the d states relative to the valence- and conduction-band levels, giving a decrease of the L-point band gaps in $Zn_{1-x}Mn_xSe$, an increase in $Zn_{1-x}Fe_xSe$, and very little change in $Zn_{1-x}Co_xSe$. The exchange interaction has a much smaller effect on the band-gap energies.

I. INTRODUCTION

Semimagnetic or diluted magnetic semiconductors (DMS's) (Refs. 1 and 2) are a class of semiconducting materials formed by randomly replacing some of the cations in a compound semiconductor with magnetic ions. Most extensively studied has been the Mn-based DMS family, in which the Mn^{2+} ($3d^5$) ion has a ${}^6S_{5/2}$ free-ion ground level. Recently, the Fe- and Co-based compounds have been synthesized and studied. The unusual electronic and optical properties of the DMS were interpreted first in terms of a (direct) sp-d exchange interaction of the form $-J\mathbf{s}\cdot\mathbf{S}$, for the coupling between the band electron spin $\mathbf{s}$ and magnetic ion spin $\mathbf{S}$.[3,4] Later, another interpretation based on p-d hybridization interaction was proposed and developed to expand the microscopic analysis of several DMS systems.[5–9]

In the $Zn_{1-x}Mn_xSe$ system, an unusual initial decrease of the fundamental band-gap energy E_0 with x has been reported[10,11] and interpreted using the exchange interaction model with a Kondo-like Hamiltonian,[12] as applied earlier to other Mn-based DMS's.[13–15] This concentration dependence of the band-gap energy in the absence of applied magnetic field is of great importance for understanding DMS heterostructures.

Recently Kim *et al.* presented a study[16] of the E_1 and $E_1+\Delta_1$ band-gap energies of $Zn_{1-x}(Mn,Fe,Co)_xSe$ showing that the sp-d exchange interaction model could marginally explain the band-gap energies of $Zn_{1-x}Mn_xSe$ but not those of $Zn_{1-x}Fe_xSe$ and $Zn_{1-x}Co_xSe$. It was suggested that to understand all three systems, the sp-d hybridization effect on the sp band structure of the host material should be considered. This effect has been applied mostly to analyze the Γ-point band gaps,[7,17,18] and to our knowledge no systematic study of this hybridization effect has yet been reported for the higher band gaps in DMS's. Higher interband transitions can yield information about the exchange interactions because they occur at positions in the Brillouin zone (BZ) offering different symmetry from that of the Γ point.

In this paper, we present a quantitative study of the sp-d hybridization effect on the energies of the E_1 and $E_1+\Delta_1$ band-gap transitions, assumed to occur at the L point of the BZ of Mn-, Fe-, and Co-doped ZnSe systems, using a semiempirical tight-binding model. In Sec. II an sp-d hybridization model Hamiltonian is derived, which consists of the host sp^3s^* bands, the impurity d states, and the interactions among them. Section III describes a quantitative application of the model to explain the reported E_1 and $E_1+\Delta_1$ band-gap energies of $Zn_{1-x}(Mn,Fe,Co)_xSe$. We conclude in Sec. IV with a brief comparison of these two different interaction mechanisms.

II. sp-d HYBRIDIZATION MODEL HAMILTONIAN

An empirical tight-binding Hamiltonian, used to study the effect of the hybridization interaction on the band-gap energies, has the form of a diluted Anderson lattice Hamiltonian and has been applied to explain mainly $Cd_{1-x}Mn_xTe$ systems.[5,6,17] In this section we rederive the formula to include more sp orbitals and justify our approximations for the small concentration range. Explicitly,

$$H=H_0+H_d+H_{sp-d}+H_{\rm ex}\ . \tag{1}$$

Here

$$H_0=\sum_{n\mathbf{k}\sigma}\varepsilon_n(\mathbf{k})c^{\dagger}_{n\mathbf{k}\sigma}c_{n\mathbf{k}\sigma} \tag{2}$$

describes the unperturbed ZnSe sp^3s^* bands using two s orbitals and six p orbitals for both cation and anion sites, including the spin-orbit interactions. Two s^* orbitals are included only to improve the description of the conduction band near the X point.[19] The operator $c^{\dagger}_{n\mathbf{k}\sigma}$ creates an electron in the Bloch state in band n, with wave number $\mathbf{k}$ and spin σ. This Bloch state can be ex-

pressed as

$$\Psi_{n\mathbf{k}}(\mathbf{r})=\frac{1}{\sqrt{N}}\sum_{\mu,s,\mathbf{R}} e^{i\mathbf{k}\cdot(\mathbf{R}+\tau_s)}C_{n\mu\sigma}(\mathbf{k})\phi_\mu(\mathbf{r}-\mathbf{R}-\tau_s)\chi_\sigma \ , \quad (3)$$

where $\phi_\mu(\mathbf{r}-\mathbf{R}-\tau_s)$ is an atomic wave function at lattice site $\mathbf{R}$ with symmetry $\mu(=s,x,y,z,s^*)$ and atomic position τ_s (=Zn or Se). χ_σ denotes the electron-spin wave function. N is the total number of lattice sites. For simplicity, we consider only nearest-neighbor interactions in H_0. The parameters $C_{n\mu\sigma}(\mathbf{k})$ are eigenvectors obtained from diagonalizing the 20×20 tight-binding Hamiltonian matrix. Since the purpose of this work is to study the effects of magnetic impurities in the small concentration range, the alloying effect is not included in this term but will be treated phenomenologically below. With the proper choice of parameters, this model yields reasonable bandwidths and wave functions for the highest valence bands and lowest conduction band, as well as band gaps in agreement with experiment.

The second term describes an effective one-electron Hamiltonian for the unperturbed localized d states of the magnetic impurity:[6,17]

$$H_d=\sum_i{}'\sum_{\nu,\sigma} n_{i\nu\sigma}(\varepsilon_d+U_{\text{eff}}\langle n_{i\nu,-\sigma}\rangle) \ , \quad (4)$$

where $n_{i\nu\sigma}$ is the number operator for d electrons in orbital ν with spin σ localized on Zn site i. The primed sum is over only those sites occupied by magnetic impurities. Implicit in this Hamiltonian is the assumption that the strongly correlated d orbital's electron-electron interaction takes the Hubbard form, U_{eff}.[6] The expectation value $\langle n_{i\nu,-\sigma}\rangle$ will be assumed to equal zero or 1. Therefore we have two fivefold d states which are separated in energy by U_{eff}. Application of the above Hamiltonian was quite successful in describing not only Mn but also more complicated Fe- and Co-based DMS systems which have minority-spin levels.[9,20] We adopted the values of U_{eff} for Mn, Fe, and Co from Ref. 9. According to the U,U',J model of Kanamori,[21,22] discussed by Hass,[18] $U_{\text{eff}}=U+4J$, $U+3J$, and $U+2J$ for Mn, Fe, and Co, respectively. The values for ε_d and U_{eff} are not sensitive to the host materials;[6] thus we can use the latest reported values for CdSe.[9] From Ref. 9, the on-site energies ε_d, which correspond to the majority-spin occupied states, are 3.4, 3.7, and 3.5 eV below the valence-band maximum of ZnSe, and U_{eff} values are 7.6, 6.8, and 5.9 eV for Mn, Fe, and Co, respectively. These relative locations of d states are important because they determine the direction of the repelling effect of hybridization. For example, concerning the conduction band at the L point, the Mn d level which lies above the L_6 conduction-band energy pushes the conduction band downward, whereas the Fe and Co d levels, which lie below the conduction band of ZnSe at the L point, push it upward. Therefore this hybridization model qualitatively explains the different behaviors observed for the three dopants.[16]

In the dilute impurity limit, when the correlation between any two localized d states can be ignored, a supercell approach is justified. We assume that the magnetic impurities of the same spin (say, spin-up) are distributed periodically, with one impurity in each supercell which has a size $1/x_\uparrow$ times that of the bulk unit cell, $x_\uparrow$ being the concentration of the spin-up impurity. Note that $x_\uparrow=x$ if all spins are aligned and $x_\uparrow=x/2$ if there are as many spin-up moments as spin-down ones. x is the total impurity concentration. We denote $\mathbf{q}$ to be a wave vector within the superlattice Brillouin zone. A Bloch state constructed from the d orbitals is given as

$$\Psi^{(d)}_{\nu\mathbf{q}}(\mathbf{r})=\frac{1}{\sqrt{N_d}}\sum_i e^{i\mathbf{q}\cdot\mathbf{R}_i}\phi^{(d)}_\nu(\mathbf{r}-\mathbf{R}_i) \ , \quad (5)$$

where $\phi^{(d)}_\nu(\mathbf{r}-\mathbf{R}_i)$ is a d-wave function for the magnetic impurity atom at cation site i, with ν labeling the five d orbitals, of symmetry $t_{2g}(xy,yz,zx)$ or $e_g(x^2\text{-}y^2,3z^2\text{-}r^2)$. We find that the e_g orbitals, which had no effect on the Γ-point study,[7] make a significant contribution to the hybridization calculation at the L point. The sum is only over states occupied by magnetic impurities of a given spin, whose total number is $N_d^\uparrow$ or $N_d^\downarrow$. Here we consider only the ferromagnetic ($N_d^\uparrow=N_d, N_d^\downarrow=0$) or paramagnetic ($N_d^\uparrow=N_d^\downarrow=N_d$) cases. The ferromagnetic (paramagnetic) case applies when an external magnetic field is applied (absent).

The third term

$$H_{sp\text{-}d}=\sum_{\nu,\mathbf{q},\sigma}\sum_{n,\mathbf{k}}[\langle\nu\mathbf{q}\sigma|V_{sp\text{-}d}|n\mathbf{k}\rangle d^\dagger_{\nu\mathbf{q}\sigma}c_{n\mathbf{k}\sigma}+\text{H.c.}] \quad (6)$$

describes magnetic impurity $3d$-Se $4sp$ hybridization, where $d^\dagger_{\nu\mathbf{q}\sigma}$ creates a d electron in the Bloch state $\Psi^{(d)}_{\nu\mathbf{q}}$ with spin σ. This hybridization interaction yields a shift of the sp band energies and a broadening of the d levels. The interaction matrix $\tilde{V}_{sp\text{-}d}$ is given by

$$\begin{aligned}\langle\nu\mathbf{q}\sigma|V_{sp\text{-}d}|n\mathbf{k}\rangle&=\frac{1}{\sqrt{NN_d}}\sum_{\mu,s,\mathbf{R},i} e^{-i\mathbf{k}\cdot(\mathbf{R}+\tau_s)+i\mathbf{q}\cdot\mathbf{R}_i}C^*_{n\mu\sigma}(\mathbf{k})\int\phi_\mu(\mathbf{r}-\mathbf{R}-\tau_s)V_{sp\text{-}d}\phi^{(d)}_\nu(\mathbf{r}-\mathbf{R}_i)d^3r\,\delta_{\mathbf{k},\mathbf{q}+\mathbf{G}_l}\\&=\left[\frac{N_d}{N}\right]^{1/2}\sum_{\mu,j} e^{i\mathbf{k}\cdot\tau_j}C^*_{n\mu\sigma}(\mathbf{k})\int\phi_\mu(\mathbf{r}-\tau_j)V_{sp\text{-}d}\phi^{(d)}_\nu(\mathbf{r})d^3r\,\delta_{\mathbf{k},\mathbf{q}+\mathbf{G}_l} \ , \end{aligned} \quad (7)$$

where $\mathbf{G}_l$ ($l=1,\ldots,N/N_d$) is a superlattice reciprocal-lattice vector enclosed within the bulk Brillouin zone, and summation j is over nearest four Se atoms around a given impurity atom. We obtain a concentration-dependent hybridization parameter governed by the factor $\sqrt{N_d/N}=\sqrt{x}$ for the ferromagnetic case and $\sqrt{N_d/N}=\sqrt{x/2}$ for the paramagnetic case. The hopping integral in Eq. (7),

$$\int \phi_\mu(\mathbf{r}-\tau_j)V_{sp\text{-}d}\phi_\nu^{(d)}(\mathbf{r})d^3r \equiv V_{\mu\nu}^{(d)} , \quad (8)$$

can be related to interaction parameters[23] $V_{pd\sigma}$, $V_{pd\pi}$, and V_{sd}, which in turn are determined by fitting experimental data. The hybridization interaction in Eq. (8) connects sp orbitals on Se sites with d orbitals (of Mn, Fe, and Co atoms) on Zn sites in the off-diagonal elements in our model Hamiltonian. The s^*-d interactions are not included, because the s^* orbitals make little contribution to the lowest conduction band near the L point.

From Eq. (7), we see that each impurity Bloch state at a fixed wave vector $\mathbf{q}$, $|\nu\mathbf{q}\sigma\rangle$ (occupied or unoccupied), is coupled to $20(N/N_d)$ bulk states labeled by $|n\mathbf{k}\rangle$ with $\mathbf{k}=\mathbf{q}+\mathbf{G}_l[n=1,\ldots,20; l=1,\ldots,(N/N_d)]$, while there is no direct coupling between bulk states $|n\mathbf{k}\rangle$ at different $\mathbf{k}$. Each bulk state at fixed wave vector, $\mathbf{k}=\mathbf{q}+\mathbf{G}_l$, is coupled directly to five (ten) occupied impurity Bloch states $|\nu\mathbf{q}\sigma\rangle$ and five (ten) unoccupied impurity Bloch states $|\nu\mathbf{q}-\sigma\rangle$ of opposite spin for ferromagnetic (paramagnetic) case ($\nu=1,\ldots,5; \sigma=\pm\frac{1}{2}$). The bulk state is coupled indirectly to other bulk states with $\mathbf{k}$ differing by a reciprocal-lattice vector $\mathbf{G}_l$ only via second-order effects. In principle, we can diagonalize a Hamiltonian matrix of dimension $[20(N/N_d)+10]$ ($[20(N/N_d)+20]$) for the ferromagnetic (paramagnetic) case to obtain the total-energy shift of the bulk band structure due to the sp-d hybridization and the cubic splitting of impurity levels. After diagonalization, we will obtain the first-order effect of impurity states on the bulk bands, and the second-order effect due to the impurity-state-mediated coupling between bulk states of different $\mathbf{k}$, separated by reciprocal-lattice vectors. However, for the purpose of getting an approximate shift of band-gap energies in the first order, it suffices to ignore the second-order effects (i.e., the indirect coupling between bulk states with the wave vector differing by a superlattice reciprocal-lattice vector). In this case, we can reduce the size of the Hamiltonian matrix by including the bulk bands of interest (namely the heavy hole, light hole, and conduction band with spin degeneracy) at a given wave vector $\mathbf{k}$, and the Bloch states constructed by impurity orbitals at a wave vector $\mathbf{q}$ which is equal to $\mathbf{k}$ shifted by an appropriate $\mathbf{G}_l$ such that $\mathbf{q}$ falls inside the superlattice Brillouin zone. Thus the rank of the Hamiltonian matrix to be diagonalized is only $6+10=16$ ($6+20=26$) for the ferromagnetic (paramagnetic) case. With this approximation, the calculation can be performed for any real value of x, whereas the full calculation can only be performed for integer values of $1/x$. The cubic crystal-field splitting of d orbitals obtained from diagonalizing this reduced Hamiltonian matrix is underestimated. However, their effects on the shift of band gaps are second order, as discussed, and can be ignored.

The final term in Eq. (1) describes the sp-d exchange interaction and can be expressed as[3,4]

$$H_{\text{ex}}=\sum_n J(\mathbf{r}-\mathbf{R}_n)\mathbf{s}\cdot\mathbf{S}_n , \quad (9)$$

where $J(\mathbf{r}-\mathbf{R}_n)$ is the ordinary exchange integral for an sp^3s^* band electron of the host ZnSe with spin $\mathbf{s}$ at $\mathbf{r}$ and a d electron of magnetic ion with spin $\mathbf{S}_n$ at $\mathbf{R}_n$. Since $Zn_{1-x}(Mn,Fe,Co)_xSe$ samples show paramagnetic behavior at room temperature,[16] the first-order perturbation given by this term, which is proportional to the thermal average of S_n^z is zero in the absence of an external magnetic field. Therefore a second-order perturbation theory within the $\mathbf{k}\cdot\mathbf{p}$ method was developed[13–15] and applied to the $Zn_{1-x}Mn_xSe$ system to explain the initial decrease of the $E_0(x)$ band gap due to the exchange interaction. The theory predicted[12] a splitting between heavy- and light-hole bands at the top of the valence band at $\mathbf{k}=0$. This result is unphysical because the p-d exchange interaction should not affect the symmetry of the crystal in the absence of the external field. The crucial approximation in this exchange interaction model[12] is that the $\mathbf{k}$-independent Γ-point ($\mathbf{k}=0$) wave function was assumed to be valid up to the nonzero cutoff wave vector $\mathbf{q}_0$. Due to valence-band degeneracy, when $\mathbf{k}$ is nonzero, there is a strong $\mathbf{k}$-dependent mixing of those valence-band wave functions defined at the Γ point ($\mathbf{k}=0$).[24] Therefore the above assumption should not be true. This discrepancy has been resolved by Ryabchenko, Semenov, and Terletskii[25] using a Green's function method which considers the fluctuations in the local concentrations of the magnetic ions and $\mathbf{k}$-dependent exchange constants. This approximation worked well for the study of the E_1 band gap[16] because the wave functions near the L point are not sensitive to $\mathbf{k}$.

III. ESTIMATION FOR L-POINT BAND GAPS OF $Zn_{1-x}(Mn,Fe,Co)_xSe$

Now we apply the model Hamiltonian we developed in Sec. II to calculate the concentration dependence of the E_1 and $E_1+\Delta_1$ band-gap energies of $Zn_{1-x}(Mn,Fe,Co)_xSe$ alloys in the absence of an external magnetic field.

As the first step, the sp^3s^* band structure of ZnSe is calculated to obtain coefficients of Bloch states in Eq. (3). We consider only nearest-neighbor interactions, and H_0 is then characterized by 13 Slater-Koster parameters[26] including three sps^* on-site energies for each cation and anion. For the hopping parameter between nearest-neighbor cation and anion sites, seven parameters are needed to express ss, sp, ps, $pp\sigma$, $pp\pi$, s^*p, and ps^* connections. With the choice of these parameters tabulated in Table I, the resulting room-temperature band structure shown in Fig. 1 describes both the top valence bands and the bottom of the conduction band of ZnSe quite satisfactorily. The spin-orbit interaction is included with two more parameters λ_a and λ_c. $\lambda_{a,c}=\Delta_{a,c}/3$, where Δ_a and Δ_c are the "renormalized" atomic spin-orbit splitting of the anion and cation p states.[27] As shown in Table II, the calculated band gaps and their spin-split gaps are in excellent agreement with the reported ones[28] both at Γ and L points.

The second step is to determine atomic sp-d hybridization parameters ($V_{pd\sigma}$, $V_{pd\pi}$, and V_{sd}). To accomplish this we used the reported value of the splitting of the valence-band edge at the Γ point in an external magnetic field. The energy splitting can be expressed by the experi-

TABLE I. Tight-binding parameters (in eV) for the band structure of ZnSe. The V_{ac} parameter denotes the atomic hybridization matrix element between the orbitals on the Se (a) and Zn (c) sites.

$E_s^{(a)}$	$E_p^{(a)}$	$E_{s^*}^{(a)}$	$E_s^{(c)}$	$E_p^{(c)}$	$E_{s^*}^{(c)}$
−11.8383	1.5072	7.5872	0.0183	5.9928	8.9928
V_{ss}	V_{sp}	V_{ps}	$V_{pp\sigma}$	$V_{pp\pi}$	
−1.5541	1.5147	2.7111	3.8872	−0.7472	
V_{ss^*}	V_{s^*s}	λ_a	λ_c		
1.1211	−1.7118	0.141	0.137		

mentally determined exchange constants (α and β) which are reasonably insensitive to x,[6]

$$\Delta E^c = xN\alpha\langle S_z\rangle \quad \text{and} \quad \Delta E^v = xN\beta\langle S_z\rangle \tag{10}$$

for conduction and valence bands, respectively. Since no room-temperature data for α and β are available, we use low-temperature data with the approximation that $\langle S_z\rangle = \frac{5}{2}$, 2, and $\frac{3}{2}$ for Mn, Fe, and Co, respectively, at $x = 0.1$. There is some variation in the reported values of α and β, and therefore we have chosen the average of the reported ones in $Zn_{1-x}Mn_xSe$,[10,29,30] $Zn_{1-x}Fe_xSe$,[31,32] and $Zn_{1-x}Co_xSe$ (Refs. 20 and 33) systems. The on-site energies and U_{eff} values for d states are chosen based on the latest values reported in Ref. 9, as discussed in Sec. II. To reproduce the splittings [Eq. (10)] in our calculation, the applied magnetic-field effect on the band structure is modeled as a sp-d hybridization effect between those sp^3s^* band states and localized d states having the same spin states. We chose $V_{pd\sigma}$ to be the only adjustable parameter, relating $V_{pd\pi}$ and V_{sd} to $V_{pd\sigma}$ by use of Harrison's ratio ($V_{sd} = 1.07V_{pd\sigma}$, $V_{pd\pi} = -1/\sqrt{3}V_{pd\sigma}$).[23] The values obtained for $V_{pd\sigma}$ are −1.267, −1.148, and −1.083 eV for Mn-, Fe-, and Co-doped ZnSe systems, respectively. The ratios of $V_{pd\sigma}$ between Mn, Fe, and Co

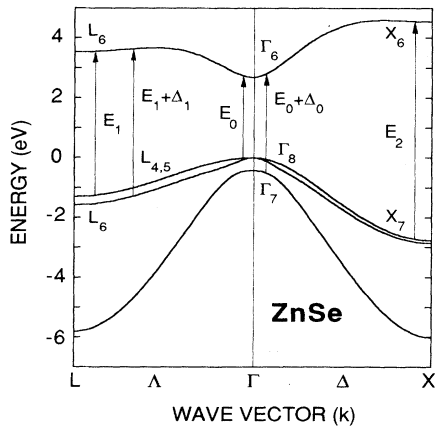

FIG. 1. ZnSe band structure calculated by the tight-binding method using the parameters in Table I. Arrows indicate several interband transitions.

TABLE II. Comparison of the band gaps calculated using the tight-binding method with experimental values reported in Ref. 28.

	Tight binding	Ellipsometry
E_0	2.6897	2.69
$E_0+\Delta_0$	3.1102	3.11
E_1	4.8308	4.83
$E_1+\Delta_1$	5.1115	5.10

obtained in this work agree well with those reported in Ref. 9.

The final step is to calculate the effect of this hybridization interaction on the band-gap energies in the absence of an external magnetic field, using the fixed interaction parameters determined in the previous step. For this calculation the restriction of the interaction between only the same spin states should be removed. Instead, the unit supercell used to construct the Bloch state is doubled in size to accommodate equal amounts of spin-up and -down states of the magnetic impurities. With the interaction parameter values determined by the Γ-point ($\mathbf{k}=\mathbf{0}$) studies above, the model Hamiltonian is calculated along the (111) direction. The advantage of this method is that we can calculate band structure at any $\mathbf{k}$ point. The effect of V_{sd} turns out to be very important at the L-point [$\mathbf{k}=(0.5,0.5,0.5)2\pi/a$] band gap. Such s-d hybridization has been neglected in the E_0 band-gap studies because it makes no contribution at the Γ point due to the tetrahedral symmetry. However, since the s-d hybridization is no longer canceled by symmetry at $\mathbf{k}\neq\mathbf{0}$, the effect of V_{sd} should not be neglected. Figure 2 shows the change in energy of the lowest conduction band and highest valence band due to the sp-d hybridization effect

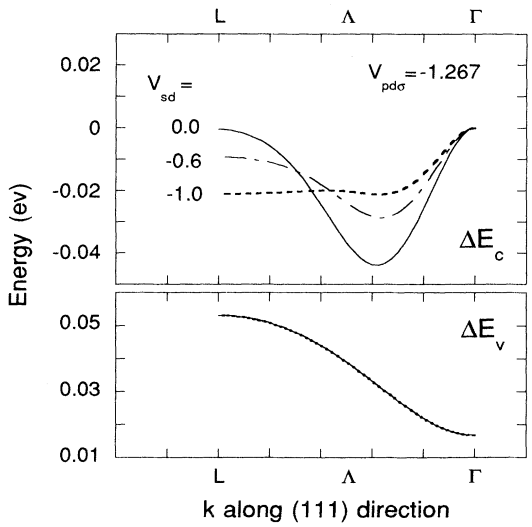

FIG. 2. The sp band energy change produced by the sp-d hybridization effect for conduction (upper) and valence (lower) bands along the [111] direction. The s-d hybridization has little effect on the valence band, while it changes the conduction band drastically. We plot with fixed $V_{pd\sigma} = -1.267$ eV to show the effect of varying V_{sd}.

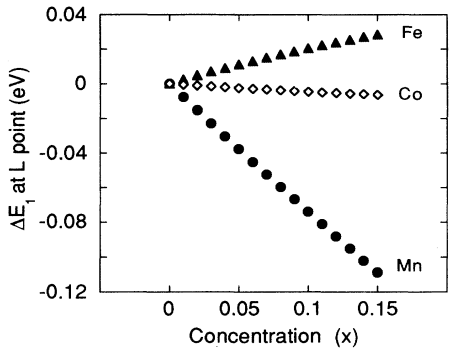

FIG. 3. Concentration dependence of the calculated *sp-d* hybridization interaction energy, $\Delta E_{sp\text{-}d}$ in eV, for $Zn_{1-x}Mn_xSe$ (filled circles), $Zn_{1-x}Fe_xSe$ (filled triangles), and $Zn_{1-x}Co_xSe$ (open diamonds).

along the (111) direction. The values of V_{sd} have little effect on the valence band (lower panel), since that band consists of mostly *p*-like states. The cancellation of the *s-d* hybridization effect in the conduction band at $\mathbf{k}=\mathbf{0}$ is also easily seen in the upper panel. However, away from $\mathbf{k}=\mathbf{0}$, the crystal symmetry no longer produces a cancellation of the effect of V_{sd}. The same behavior is also seen for Fe and Co calculations.

When the conduction (Λ_6^c) and valence ($\Lambda_{4,5}^v, \Lambda_6^v$) bands are nearly parallel, the E_1 and $E_1+\Delta_1$ band gaps receive contributions not only from the L point but also from the Λ bands.[34–36] In ZnSe, however, since the Λ bands are nearly parallel only in a region close to the L point,[16] we consider only the L-point contribution to simplify the calculation. The calculated change in the E_1 band-gap energy ($\Delta E_{sp\text{-}d}$) due to the *sp-d* hybridization effect at the L point as a function of x is shown in Fig. 3. Recall the case of Fe, in the *sp-d* direct exchange interaction model,[16] where the slope was negative. The slope for Fe now is positive, and the earlier model's large negative slope for Co now becomes almost zero, in agreement with the reported data.[16]

For further quantitative analysis, the alloying effect is approximated by adding a linear-dependent term [Dx, where $D=0.2$ eV (Ref. 30)] to the calculated sp^3s^* band gaps of ZnSe as a perturbation. Final estimates of the E_1 and $E_1+\Delta_1$ band gaps along with the reported[16] experimental data are shown in Fig. 4. Even though there are some discrepancies in the $E_1+\Delta_1$ band gaps, judging from the fact that our model used parameters fixed from other experiments without any further adjustments, it remarkably appears to explain the different behaviors of concentration-dependent band-gap energies in the three Mn-, Fe-, and Co-doped ZnSe systems.

IV. CONCLUDING REMARKS

The *sp-d* exchange interaction model was widely used in the past to explain concentration- and temperature-dependent band-gap energies of several DMS systems,[12,37,38] assuming[3,4] that the experimentally measured exchange integral β [defined in Eq. (10)] is due entirely to direct exchange interaction. Recently, another interpretation which describes β as fully arising from the *p-d* hybridization interaction was proposed and developed.[5–9] Since both exchange and hybridization interactions coexist in the total system Hamiltonian of Eq. (1), the effects of both interactions should be added to describe the *d* electron effects on the L-point band-gap energies of the system. Our calculation in this paper shows that only the hybridization interaction effect is strong enough to explain the observed concentration dependence of the L-point band gaps of all $Zn_{1-x}Mn_xSe$, $Zn_{1-x}Fe$,Se, and $Zn_{1-x}Co_xSe$ systems. The exchange interaction alone, however, could marginally explain the L-point band gaps of the $Zn_{1-x}Mn_xSe$ system.[16] In Ref.

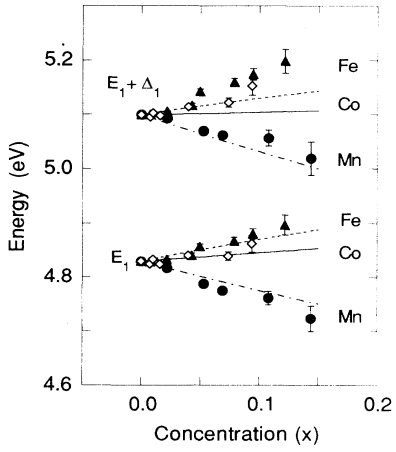

FIG. 4. Estimated concentration-dependent band-gap energies of our model are shown as lines for $Zn_{1-x}Mn_xSe$ (dot-dashed line), $Zn_{1-x}Fe_xSe$ (dotted line), and $Zn_{1-x}Co_xSe$ (solid line). Symbols represent the experimental data of Ref. 16.

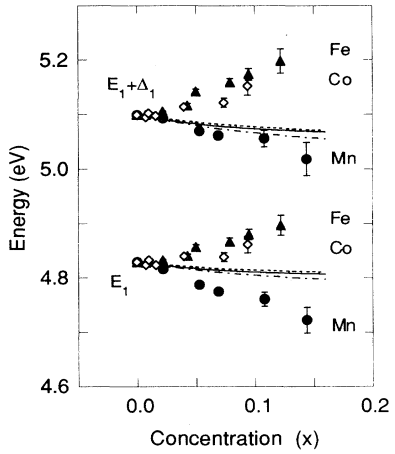

FIG. 5. Estimated concentration-dependent band-gap energies predicted with the exchange interaction model are shown as lines for $Zn_{1-x}Mn_xSe$ (dot-dashed line), $Zn_{1-x}Fe_xSe$ (dotted line), and $Zn_{1-x}Co_xSe$ (solid line). Symbols represent the data of Ref. 16. We used $D=0.1$ eV, and $q_0=3.3\times10^7$ cm^{-1} in Eq. (11) of Ref. 16.

16, the cutoff wave vector q_0 value used to predict the band gaps of $Zn_{1-x}Mn_xSe$ is 6.6×10^7 cm^{-1}, which is 0.6 of the distance to the Brillouin-zone (BZ) boundary. Even though a similar value was reported in the $Cd_{1-x}Mn_xTe$ system ($q_0=6.6\times10^7$ cm^{-1}),[37] this value is too large to be consistent with the perturbation theory of the exchange interaction model. When we use a more reasonable value such as $q_0=3.3\times10^7$ cm^{-1}, which is 0.3 of the BZ, the estimates using the exchange interaction model appear as in Fig. 5, which clearly shows that the effect of the interaction is too small to explain any results on the Zn_{1-x}(Mn,Fe,Co)$_x$Se system. (Furthermore, if we use values of theoretical exchange interaction parameters at the L point interpreted by the hybridization model,[39] the estimation in Fig. 5 comes out to be an order of magnitude smaller.) This estimation is reasonable, because the exchange interaction should be smaller by an order of magnitude than that from the hybridization for the following reasons. As shown in Sec. II, the effect of exchange interaction on the band-gap energies is of second order, while that of hybridization is of first order. We also interpret that the former can be considered to be the scattering of the band electrons by the impurity d electrons (two-electron system), whereas the latter determines the appropriate one-particle states for interacting sp band states and localized d states within the Hartree-Fock theory. Therefore we conclude that the sp-d interaction in these DMS materials is to be interpreted as a hybridization interaction whose strength is much larger by an order of magnitude than that of the exchange interaction. However, this quantitative agreement between our analysis and the data should be taken carefully since there are considerable uncertainties in the interpretation of the photoemission data,[9] in particular the position of the d levels and the values of U_{eff}. More systematic studies, such as temperature- and magnetic-field-dependent experiments on the E_1 and $E_1+\Delta_1$, as well as on the E_0 and $E_0+\Delta_0$ band gaps, should be done to confirm our analysis.

ACKNOWLEDGMENT

This work was supported by NSF through the University of Illinois, Materials Research Laboratory under Contract No. NSF DMR 89-20538.

[1]N. B. Brandt and V. V. Moshchkalov, Adv. Phys. **33**, 193 (1984).
[2]J. K. Furdyna and J. Kossut, in *Semiconductors and Semimetals,* edited by R. K. Willardson and A. C. Beer (Academic, San Diego, 1988), Vol. 25.
[3]J. Kossut, Phys. Status Solidi B **78**, 537 (1976).
[4]G. Bastard, C. Rigaux, and A. Mycielski, Phys. Status Solidi B **79**, 585 (1977).
[5]A. K. Bhattacharjee, G. Fishman, and B. Coqblin, Physica **117B&118B**, 449 (1983).
[6]B. E. Larson, K. C. Hass, H. Ehrenreich, and A. E. Carlsson, Phys. Rev. B **37**, 4137 (1988).
[7]P. M. Hui, H. Ehrenreich, and K. C. Hass, Phys. Rev. B **40**, 12 346 (1989).
[8]J. Masek, Solid State Commun. **78**, 351 (1991).
[9]A. K. Bhattacharjee, Phys. Rev. B **46**, 5266 (1992).
[10]A. Twardowski, T. Dietl, and M. Demianiuk, Solid State Commun. **48**, 845 (1983).
[11]K. J. Ma and W. Giriat, Phys. Status Solidi A **95**, K135 (1986).
[12]R. B. Bylsma, W. M. Becker, J. Kossut, and U. Debska, Phys. Rev. B **33**, 8207 (1986).
[13]F. Rys, J. S. Helman, and W. Baltensperger, Phys. Konden. Mater. **6**, 105 (1967).
[14]C. Hass, Phys. Rev. **168**, 531 (1968).
[15]J. Diouri, J. P. Lascaray, and M. E. Amrani, Phys. Rev. B **31**, 7795 (1985).
[16]Y. D. Kim, S. L. Cooper, M. V. Klein, and B. T. Jonker, Phys. Rev. B (to be published).
[17]K. C. Hass and H. Ehrenreich, Acta Phys. Pol. A **73**, 933 (1988).
[18]K. C. Hass, in *Semimagnetic Semiconductors and Diluted Magnetic Semiconductors,* edited by M. Averous and M. Balkanski (Plenum, New York, 1991), p. 59.
[19]P. Vogl, H. P. Hjalmarson, and J. D. Dow, J. Phys. Chem. Solids **44**, 365 (1983).
[20]J. P. Lascaray, F. Hamdani, D. Coquillat, and A. K. Bhattacharjee, J. Magn. Magn. Mater. **104-107**, 995 (1992).
[21]J. Kanamori, Prog. Theor. Phys. **30**, 275 (1963).
[22]B. H. Brandow, Adv. Phys. **26**, 651 (1977).
[23]W. A. Harrison, *Electronic Structure and the Properties of Solids* (Dover, New York, 1989).
[24]J. M. Luttinger and W. Kohn, Phys. Rev. **97**, 869 (1956).
[25]S. M. Ryabchenko, Y. G. Semenov, and O. V. Terletskii, Phys. Status Solidi B **144**, 661 (1987).
[26]J. C. Slater and G. F. Koster, Phys. Rev. **94**, 1498 (1954).
[27]D. J. Chadi, Phys. Rev. B **16**, 790 (1977).
[28]Y. D. Kim, S. L. Cooper, M. V. Klein, and B. T. Jonker, Appl. Phys. Lett. **62**, 2387 (1993).
[29]A. Twardowski, M. V. Ortenberg, M. Demianiuk, and R. Pauthenet, Solid State Commun. **51**, 849 (1984).
[30]J. K. Furdyna, J. Appl. Phys. **64**, R29 (1988).
[31]A. Twardowski, P. Glod, W. J. M. de Jonge, and M. Demianiuk, Solid State Commun. **64**, 63 (1987).
[32]X. Liu, A. Petrou, B. T. Jonker, G. A. Prinz, J. J. Krebs, and J. Warnock, Appl. Phys. Lett. **53**, 46 (1988).
[33]X. Liu, A. Petrou, B. T. Jonker, J. J. Krebs, G. A. Prinz, and J. Warnock, J. Appl. Phys. **67**, 4796 (1990).
[34]F. H. Pollak and M. Cardona, Phys. Rev. **172**, 816 (1968).
[35]S. Koeppen, P. Handler, and S. Jasperson, Phys. Rev. Lett. **27**, 265 (1971).
[36]D. E. Aspnes and J. E. Rowe, Phys. Rev. B **7**, 887 (1972).
[37]J. A. Gaj and A. Golnik, Acta Phys. Pol. A **71**, 197 (1987).
[38]L. Bryja and J. A. Gaj, Acta Phys. Pol. A **73**, 459 (1988).
[39]A. K. Bhattacharjee, in *Proceedings of the International Conference on the Physics of Semiconductors, Thessaloniki, Greece,* edited by E. M. Anastassakis and J. D. Joannopoulos (World Scientific, Singapore, 1990), p. 763.